High β, long pulse, bootstrap sustained scenarios on the National Spherical Torus Experiment (NSTX)*

D. A. Gates†, for the NSTX National Research Team

†*Plasma Physics Laboratory, Princeton University, P.O.Box 451, Princeton, New Jersey 08543*

Abstract

Long pulse, high β scenarios have been established on NSTX [1]. $\beta_t(\equiv 2\mu_0\langle P\rangle/B_{t0}^2) \sim 35\%$ has been achieved during transient discharges. The machine improvements that lead to these results, including error field reduction and high temperature bakeout of plasma facing components are described. The highest β_t plasmas have high triangularity ($\delta = 0.8$) and elongation ($\kappa = 2.0$), at low aspect ratio $A \equiv R/a = 1.4$. The strong shaping permits large values of normalized current, $I_N(\equiv I_p/(aB_{t0})) \approxeq 6$ while maintaining moderate values of $q_{95} = 4$. Long pulse discharges up to 1s in duration have been achieved with substantial bootstrap current. The total non-inductive current drive can be as high as 60%, comprised of 50% bootstrap current and $\sim 10\%$ neutral beam current drive. The confinement enhancement factor H_{89P} is in excess of 2.7. $\beta_N * H_{89P} \gtrsim 15$ has been maintained for $8 * \tau_E \sim 1.6 * \tau_{CR}$, where τ_{CR} is the relaxation time of

the first radial moment of the toroidal current density. The ion temperature for these plasmas is significantly higher than that predicted by neoclassical theory.

I. Introduction

The theoretically predicted advantages of the spherical torus (ST) concept are well known [2]. Since the achievement of high $\beta_t \sim 34\%(\equiv 2\mu_0\langle P\rangle/B_{t0}^2)$ with good confinement on the Small Tight Aspect Ratio Tokamak (START) device [3, 4], the pace of ST research has increased rapidly. The achievement of high β_t (which on START eventually reached 40% [5]) is crucial to the success of the ST as a reactor concept since the demanding geometric constraints combined with the rigors of the intense neutron environment in the core of such a device nearly preclude the use of super-conducting toroidal field (TF) coils. Therefore, in order to compete with the ohmic losses in the normal conducting TF magnet, the fusion power density in an ST must be high. Similarly, the same constraints all but rule out the inclusion of an internal transformer solenoid coil. Theoretical work [6, 7] has indicated the existence of equilibria which are both magneto-hydrodynamically (MHD) stable (in the presence of a perfectly conducting wall) and which have a self-consistent bootstrap current profile which can provide $\sim 100\%$ of the plasma current at high β.

The National Spherical Torus Experiment (NSTX) [1] is a mid-size device designed to demonstrate the relevant fusion energy science of the ST on the

proof-of-principle scale. Recent improvements to NSTX will be described in section II. An important part of the NSTX mission is to demonstrate the physics basis required to verify the existence of high β, self-sustained discharges. Toward this goal, recent experiments have achieved $\beta_t = 35\%$ during transient discharges, the results of which will be described in sections III and IV. Additionally, plasmas have been created with overall pulse length of $\gtrsim 1s$ at high normalized $\beta(\equiv \beta_t a B_{t0}/I_p)$ where a is the plasma minor radius and $\beta_t = 15\%$ with confinement times ~ 2.7 times those predicted by the ITER89P scaling. The properties of these long pulse discharges will be discussed in sections V and VI.

II. Machine Improvements

Several changes to the NSTX device were key to achieving high performance discharges on NSTX. One of the most important was the correction of the error field caused by a manufactured defect in the vertical field coil (see Figure 2 for coil location). The correction of this error has led to a reduction of the occurrence of non-rotating MHD modes on NSTX [8]. Previously, at high β, non-rotating MHD modes were often seen as precursors to a loss of plasma confinement [9]. In addition, the circuit driving the inner divertor coil (see 2 for coil location) was modified to minimize the current ripple in

this coil. The inner divertor coil allows for creation of high triangularity discharges, which is important for achieving high β_t.

Previously, H-mode plasmas on NSTX [10] were not achieved reliably. This situation has been alleviated by the commissioning of a system for high temperature ($350°C$) bake-out of plasma facing components as well as the addition of gas fuelling from the high field side of the plasma. High temperature bake-out is a well established technique for conditioning carbon plasma facing components. The addition of a high field side fuelling capability was prompted by the observation on the Mega-Amp Spherical Tokamak (MAST) device [11] that such a fuelling port improved the reliability of achieving H-mode [12].

III. High β plasmas - effect of shaping

The time history of a typical high β_t discharge is shown in Figure 1. The plasma current is ramped up at a rate of 5MA/s. Neutral beam heating ($\sim 1.7MW$) is applied early in the discharge to help heat the plasma and to slow the relaxation of the current profile. An additional 3.3MW of neutral beam heating power is applied at the start of the plasma current flattop. Shown in Figure 2 is a plot of contours of constant poloidal flux for a plasma equilibrium that achieved $\beta_t = 35\%$ as computed by the EFIT equilbrium

reconstruction code [13, 9]. The high elongation $\kappa = 2.0$ and triangularity $\delta = 0.8$ of this discharge allow for increased plasma current ($I_p = 1.2MA$) at low toroidal field ($B_t = 0.3T$) while maintaining a moderate value for $q_{95} = 3.8$. Plasmas with high triangularity at higher toroidal field $B_t = 0.55T$ have achieved stored energies of $0.4MJ$. The neutral beam heating power on this high stored energy discharge was 7MW.

The effects of shaping on plasma β-limits in the ST configuration are similar to those found in conventional aspect ratio tokamaks, but the effects are enhanced by the stronger radial variation of the toroidal field at low aspect ratio. In particular, the vacuum toroidal field in any axi-symmetric magnetic confinement device scales as $B_0 R_0/R$, where B_0 is the vacuum magnetic field at R_0, and R is the horizontal distance from the vertical axis of symmetry. The term R_0/R varies from 4.3 to 0.56 between the high field and the low field side of a typical NSTX equilibrium. The fraction of the cross-sectional area of the plasma that is in the region of highest toroidal magnetic field increases rapidly as the plasma triangularity increases, as shown in Figure 3. Also shown in the figure are two model plasma boundaries of the form $s = [R, Z]$ where $R = R_0 + a\cos(\theta + \delta \sin\theta)$ and $Z = a\kappa \sin\theta$, where $R_0 =$ major radius of the boundary center, $a =$ minor radius of the boundary, δ

= triangularity, and κ = elongation of the boundary. These boundaries are used to calculate the quantities in Figure 4. The change in volume averaged magnetic energy density between the low and high triangularity case shown in the figure is 35% as can be seen in Figure 4. Increasing the average magnetic pressure while keeping the axial magnetic field fixed allows greater values of kinetic pressure without raising the current in the toroidal field coil. In addition to the benefit gained with δ in magnetic pressure there is also an increase in the edge safety factor with increasing triangularity. The dashed line in Figure 4 indicates the increase in q due the geometric variation of toroidal field. The increase in this parameter is 60% at the highest δ.

Shown in Figure 5 is a Troyon [14] plot showing the dependence of the achievable β_t on the normalized current ($I_N = I/aB_{t0}[MA/(m \cdot Tesla)]$). $\beta_N > 6.0$ is routinely achieved on NSTX. To date the highest β_N values have not yet been achieved at the maximum normalized current, indicating the possibility of further increases in toroidal β. Shown in Figure 6 is the same database plotted versus the original Troyon definition of $\langle\beta\rangle \equiv 2\mu_0\langle P\rangle/\langle B^2\rangle$, which uses the volume average total magnetic energy density as the normalization. The results shown in Figures 5 , 6 are interesting in several ways: 1) they show that NSTX has achieved high β, regardless of the definition

used, 2) a comparison of the two figures show that for the higher currents the poloidal field stored energy and the paramagnetic part of the total field are large relative to the vacuum toroidal field, and, most importantly, 3) that NSTX plasmas are well above the no-wall β-limit of $\langle\beta_N\rangle \sim 3$. Recent theoretical work has shown that $\langle\beta_N\rangle \sim 3$ describes the no-wall ideal MHD external kink limit for a large range of $q* \equiv \epsilon(1+\kappa^2)\pi a B_{t0}/\mu_0 I_p$ and aspect ratio, as shown in recent theoretical work [15].

An important additional factor in achieving high β on NSTX was the advent of reliable H-mode operational scenarios. The phenomenology of the H-mode on NSTX is described in [16]. However, the achievement of H-mode has an important role to play in high β, due to the much lower pressure peaking factors that are obtained in this operational regime. It has been shown previously [17] that the β-limit depends inversely on the pressure peaking factor $F_p(\equiv p(0)/\langle p\rangle)$.

IV. Stability of high β_t discharges

Many of the highest β_t discharges end in a rapid disruption. This disruption is preceded on a long timescale ($\sim 50ms$) by a large rotating $m/n = 1/1$ MHD mode. Immediately preceding the disruption the growth rate of the mode increases rapidly ($\sim 400\mu sec$). It is plausible to assume that the cause

of this rapidly growing mode is an ideal kink although, other than the large ideal-like growth rate, there is little direct supporting evidence for this assumption. The rapid disruption is likely associated with the large size of the q =1 radius of this discharge. The horizontal viewing soft X-ray data indicates that the vertical diameter of the 1/1 mode is 2.0m, with the total plasma height of 2.4m. However, for the highest beta discharge shown in Figure 1, the plasma does not end in a disruption. Rather, the large 1/1 tearing mode simply causes β saturation. This plasma is at slightly lower β_N, and the input beam power is higher. The exact dynamics which limit plasma performance at high toroidal β are shrouded by lack of information about the current profile, as evidenced by the variability of disruption behavior for discharges with similar evolutions [8].

V. High β_p discharges - long pulse

An example of the time history of a typical NSTX long pulse equilibrium is shown in Figure 7. Neutral beam preheating is applied as in the previously described high β_t scenario. The plasma makes a transition to H-mode at the time of the I_p flat-top, as evidenced by the drop in $D\alpha$ emission and remains in H-mode until the end of the discharge. This particular shot is of interest because, except for the continuing slow density rise, the plasma

reaches steady state. An equilibrium cross-section for this discharge is shown in Figure 8. The lower single null (LSN) configuration was chosen for these discharges, since a quiescent H-mode operational regime was routinely obtained in this configuration. The H-mode provides broader pressure profiles which give a better aligned bootstrap current, as well as allowing for stable operation at higher β_p. The total non-inductive current is 55%, as calculated by the TRANSP code. The bootstrap current fraction for this discharge, as calculated by the NCLASS module within TRANSP, is $\sim 40\%$. This value is mitigated by the finite electron collisionality of NSTX. The collisionless bootstrap fraction is estimated to be 60%. The collisionality peaks in the edge, so that the bootstrap current profile would be naturally broader if the electron temperature in this region were higher (for fixed β_p). The average triangularity of this discharge is $\delta \sim 0.4$, with elongation $\kappa \sim 2.0$. Higher δ was found to be beneficial in the LSN discharges, similar to the highly shaped double null discharges described in section 3. However, there was an apparent trade off between maximizing the triangularity and optimizing the access to the quiescent H-mode. The cause of this effect is under investigation.

The β_N is ~ 5.5, with $\langle \beta_N \rangle \sim 4$. This value is calculated to be $\sim 20\%$ above the ideal no-wall n=1 external kink limit by the DCON [18] stability

code. The plasma shows no sign of disruptive MHD of any kind for $\sim 400ms$ which is at least $\sim 20 * \tau_{wall}$, where τ_{wall} is the decay time of the eddy current induced in the conducting structure by the MHD mode as calculated by the VALEN [19] code. Shown in Figure 9 is the stability parameter δW as calculated by DCON (a negative value indicates instability). As can be seen in the Figure, the plasma β_N exceeds the no-wall limit at $t = 320ms$ while the ideal with-wall criterion is never violated, indicating the conducting structure in NSTX is stabilizing the external kink.

VI. Confinement

The energy global confinement time of the discharge shown in Figure 7 is 54ms, without correcting for beam losses or fast particle stored energy, and is steady at this value for $8 * \tau_E$. The confinement time predicted by the ITER89P [20] scaling relation is 20ms, giving $H_{89P} \sim 2.7$. As stated earlier, $\beta_N \sim 5.5$, giving a product $\beta_N * H_{89P} \sim 15$. This quantity is a popular parameter for determining how advanced a tokamak discharge is, as it is a normalized version of the ignition criterion at fixed q_{95}. A plot of this parameter vs. the number of energy confinement times for which the stored energy remained constant is shown in Figure 10. For reference, an outline of the operating space for the conventional aspect ratio advanced tokamak

is shown in the figure. Another parameter which has received attention as a figure of merit is $\beta_N H89/q_{95}^2$, sometimes referred to as the ITER ignition figure of merit. Shot 108730 achieves a peak value 0.37, which is quoted for lack of a viable normalized ignition parameter that is independent of aspect ratio.

The timescale of these long-pulse discharges is not only long relative to the energy confinement time, it also is long relative to the current relaxation time. The current penetration time for the plasma shown in Figure 7 is $\sim 250ms$. Therefore the plasma persists for $1.6 * \tau_{CR}$, where τ_{CR} is the relaxation time of the first radial moment of the toroidal current density. This is an even more relevant normalization for pulse length than the energy confinement time, since it indicates that the current profile has begun to come into equilibrium.

The single fluid thermal diffusivity profile for the plasma discharge as in Figure 7 is shown in Figure 11. The single fluid thermal diffusivity is $\chi_{eff} \sim 2m^2/s$, where $\chi_{eff} \equiv \Gamma_{tot}/\nabla(T_e + T_i)$, similar in value to a conventional tokamak with comparable plasma parameters. Also shown in the figure is the predicted (Chang-Hinton) ion neoclassical diffusivity for the same discharge as well as the χ_i as calculated by the NCLASS code. The diffussivity

values are very similar indicating that the single fluid confinement is excellent - on the order of the ion neoclassical value. The picture becomes even more interesting when the ions and electrons are considered separately. Shown in Figure 12 is the ion temperature calculated using $\chi_i = \chi_{i(Chang-Hinton)}$ as well as using $\chi_i = 0.001 * \chi_{i(Chang-Hinton)} \sim 0$, along with the measured ion and electron temperatures. As is apparent from the figure the ion temperature exceeds that predicted using either of the assumed diffusivities. It is important to note that this result is not ubiquitous and that there are numerous operational scenarios on NSTX that do not show this behavior. In particular, plasmas heated with High Harmonic Fast Waves [21] have $T_i < T_e$, and many beam heated discharges on NSTX have ion temperatures that are more consistent with those predicted by neoclassical theory.

The certainty in the NSTX diagnostic measurements has significantly improved recently, due to directed efforts to resolve issues related to the electron-ion power balance in NSTX plasmas. The Thomson scattering measurements of line averaged electron density and peak electron temperature have been independently verified using far infra-red interferometry and X-ray spectroscopy of Argon $n = 3$ satellite lines, respectively. Similarly, the peak ion temperature measurement has been independently verified using Doppler

X-ray spectroscopy of the same Argon lines.

This raises the question as to what is the cause of this interesting ion temperature anomaly which is evident in 12. 1) The possibility of an undiscovered systematic error in the diagnostic data cannot be ruled out. In particular, if the plasma is shifted relative to the axis of the device, the excess ion temperature could be substantially reduced. The other possibilities are numerous: 2) errors in the estimated values of unmeasured parameters used as inputs to the TRANSP code, important parameters being the edge neutral density (unmeasured) and the profile of Z_{eff} (currently only line integral value is used) 3) an imperfection in the TRANSP power balance calculation due to low aspect ratio 4) an imperfection in the beam slowing down calculation due to large gyro-orbits/ electric fields that distributes power differently between ions and electrons [one of the primary factors in creating the anomaly is the classical beam heating calculation which indicates that $\sim 2/3$ of the beam power is absorbed by the electrons] 5) an anomalous ion heating mechanism, at least one of which has been suggested [22].

VII. Summary

NSTX has established operating regimes which achieve both high toroidal β, and which have substantial non-inductive current drive. The highest

toroidal β discharges are transient, but a quiescent H-mode operational scenario with moderate toroidal $\beta \sim 16\%$ and high $\beta_p \sim 1.2$ has been sustained for $8 * \tau_E \sim 1.6\tau_{CR}$. This long pulse scenario has up to 60% non-inductive current drive with $\sim 50\%$ bootstrap fraction. β_N is maintained above the no-wall limit for many resistive wall times. The confinement in these discharges is very good, achieving H89P enhancement factors of ~ 2.7. The product of $\beta_N * H_{89P} \sim 15$ for $\sim 1.6\tau_{CR}$ is an important result for establishing the viability of a steady-state ST fusion energy device. The ion loss power in these discharges sometimes exceeds the classical ion heating as calculated by the TRANSP code, an intriguing result that is a topic of ongoing study. The single fluid diffusivity is similar to the ion neoclassical value.

The lead author would like to acknowledge individual members of the NSTX Team that have made particularly important and direct contributions. These include, J. Menard, S. Kaye, S. Sabbagh, R. Maingi, R. Bell, M. Bitter, and B. LeBlanc.

*This work was supported by the U.S. Department of Energy Grant under contract number DE-AC02-76CH03073.

References

[1] M. Ono, S. M. Kaye, Y. -K. M. Peng, *et al.*, Nucl. Fusion **40**, 557 (2000)

[2] Y-K. M. Peng and D. J. Strickler, Nucl. Fusion **26**, 769 (1986)

[3] D. A. Gates, R. Akers, L. Appel, *et al.*, Phys. Plasmas **5**, 1775 (1998)

[4] M. Gryaznevich, R. Akers, P. G. Carolan, *et al.*, Phys. Rev. Lett. **80**, 3972 (1998)

[5] A. Sykes, Nucl. Fusion **39**, 1271 (1999)

[6] J. E. Menard, S. C. Jardin, S. M. Kaye, C. E. Kessel, and J. Manickam, Nucl. Fusion **37**, 595 (1997)

[7] R. L. Miller, LinLiu YR, A. D. Turnbull, V. S. Chan, L. D. Pearlstein, O. Sauter, and L. Villard, Phys. Plasmas **4**, 1062 (1997)

[8] J. Menard, M. G. Bell, R. E. Bell, *et al.*, *β-limiting MHD instabilities in improved-performance NSTX spherical torus plasmas*, to be published in Nuclear Fusion (2003)

[9] S. A. Sabbagh, R. E. Bell, M. G. Bell, *et al.*, Phys. Plasmas **9**, 2085 (2002)

[10] R. Maingi, M. G. Bell, R. E. Bell, *et al.*, Phys. Rev. Lett. **88**, 035003-1 (2002)

[11] M. Cox, Fusion Eng. Des. **46**, 397 (1999)

[12] M. Valovic, P. G. Carolan, A. R. Field, *et al.*, Plasma Phys. Control. Fusion **44**, A175 (2002)

[13] L. L. Lao, H. St. John, R. D. Stambaugh, A. G. Kellman, and W. Pfeiffer, Nucl. Fusion **25**, 1611 (1985)

[14] F. Troyon, J. Gruber, H. Saurenmann, S. Semenzato, and S. Succi, Plas. Phys. and Controlled Fusion **26**, 209 (1984)

[15] J. E. Menard, M. G. Bell, R. E. Bell, *et al.*, *Unified Ideal Stability Limits for Advanced Tokamak and Spherical Torus Plasmas*, submitted to Phys. Rev. Lett. (2002)

[16] C. E. Bush, Bull Am. Phys. Soc. **44**, 183 (2002)

[17] S. A. Sabbagh, J. Bialek, R. E. Bell, *et al.*, *The Resistive Wall Mode and Feedback Control Physics Design in NSTX*, No. EX/S2-2, to be published in Fusion Energy (2003)

[18] A. H. Glasser, and M. S. Chance, Bull Am. Phys. Soc. **42**, 184 (1997)

[19] J. Bialek, A. H. Boozer, M. E. Mauel, and G. A. Navratil, Phys. Plasmas **8**, 2170 (2001)

[20] P. N. Yushmanov, T. Takizuka, K. S. Riedel, O. J. W. F. Kardaun, J. G. Cordey, S. M. Kaye, and D. E. Post, Fusion Technol., **30**, 1999 (1990)

[21] J.R. Wilson, Bull Am. Phys. Soc. **44**, 221 (2002)

[22] D. A. Gates, N. N. Gorelenkov, R. B. White, Phys. Rev. Lett. **87**, 205003-1 (2001)

Captions

Figure 1: Time history of high toroidal β discharge 108989. The β_t is calculated using the EFIT equilibrium fitting code. Shown in the figure is a) plasma current (MA), b) Dα emission, c) β_t from EFIT, d) injected neutral beam power.

Figure 2: Isoflux contour plot of high β_t shot 108989. The vertical field coil is the PF coil with the largest major radius, and the inner divertor coil is PF the coil with the smallest major radius.

Figure 3: Model boundary shapes at the limits of the range in δ used to calcualate the curves in Figure 4.

Figure 4: Calculated volume averaged vacuum magnetic pressure and line averaged B/R vs. δ for 2 different aspect ratios $A = 1.4$ and $A = 2.8$. All values are normalized to the value at $\delta = 0$.

Figure 5: Toroidal β vs. normalized current $I_N \equiv I_p/aB_{t0}(MA/m \cdot Tesla)$ for a database of NSTX equilibria. $\beta_N \sim 6$ is routinely achieved. The red points were taken during the 2002 operational campaign, whereas the black data are from 2001.

Figure 6: $\langle\beta\rangle \equiv 2\mu_0\langle P\rangle/\langle B^2\rangle$ vs. normalized current $I_N \equiv I_p/aB_{t0}(MA/m \cdot Tesla)$ for a database of NSTX equilibria. $\langle\beta_N\rangle \gtrsim 3$ is routinely achieved. The red points were taken during the 2002 operational campaign, whereas the black data are from 2001.

Figure 7: Time history of long pulse discharge 108730. Shown in the figure is a) plasma current (MA), b) Dα emission, c) β_p from EFIT, d) loop voltage at the inner vacuum boundary.

Figure 8: Isoflux contour plot of long pulse discharge 108730 at time t=0.51s. The equilibrium is reconstructed using the EFIT reconstruction code.

Figure 9: Output from the DCON stability code indicating that this discharge is unstable to an n=1 external kink mode in the absence of a conducting wall. The plasma remains stable in the presence of a conducting wall according to the calculation.

Figure 11: Single fluid thermal diffuesivity for the shot in Figure 7. Also shown in the plot is the Chang-Hinton predicted ion neoclassical χ_i along with χ_i as calculated using the NCLASS code.

Figure 12: Measured ion (green) and electron (red) temperatures for shot 108730, compared with 2 theoretically predicted ion temperatures a) using Chang-Hinton neoclassical thermal diffusivity (black), and b) Using 0.001*Chang-Hinton (blue).

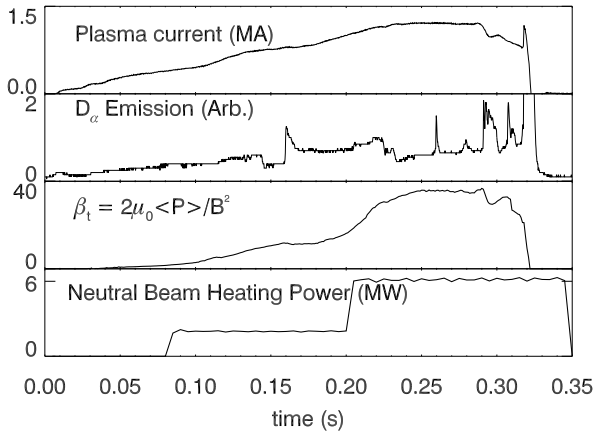
1.5
Plasma current (MA)
0.0
2
D_α Emission (Arb.)
0
40
$\beta_t = 2\mu_0 <P>/B^2$
0
6
Neutral Beam Heating Power (MW)
0
0.00
0.05
0.10
0.15
0.20
0.25
0.30
0.35
time (s)

Figure 1:

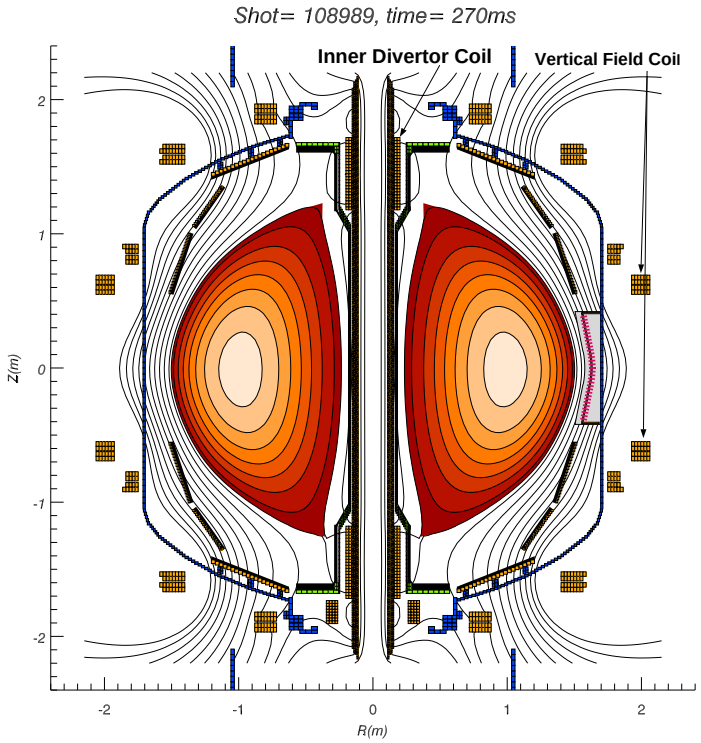
Shot= 108989, time= 270ms
Inner Divertor Coil
Vertical Field Coil
Z(m)
R(m)
2
1
0
-1
-2
-2
-1
0
1
2

Figure 2:

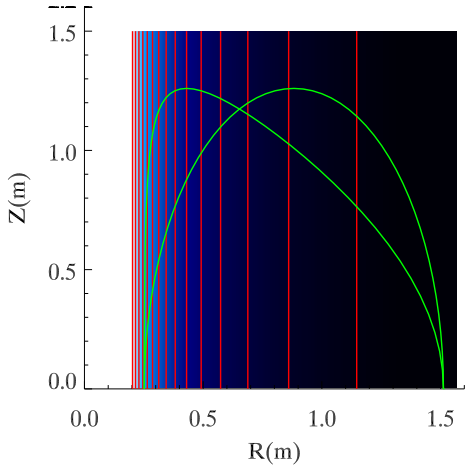

Figure 3:

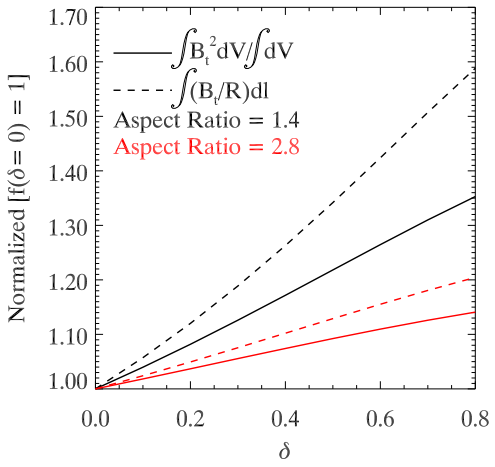
1.70
1.60
1.50
1.40
1.30
1.20
1.10
1.00
Normalized [f(δ = 0) = 1]
∫B_t^2 dV/∫dV
∫(B_t/R)dl
Aspect Ratio = 1.4
Aspect Ratio = 2.8
0.0
0.2
0.4
0.6
0.8
δ

Figure 4:

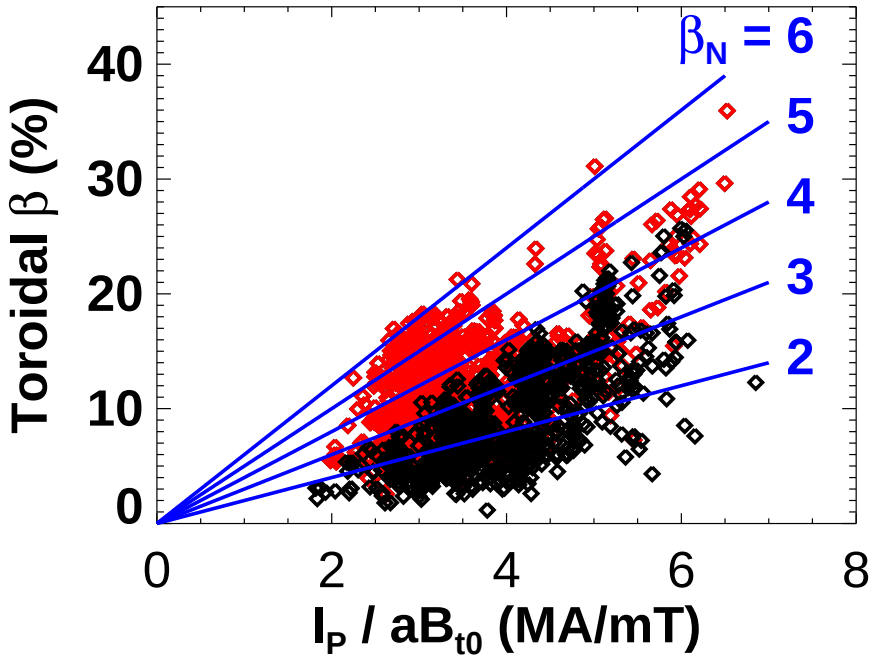

Figure 5:

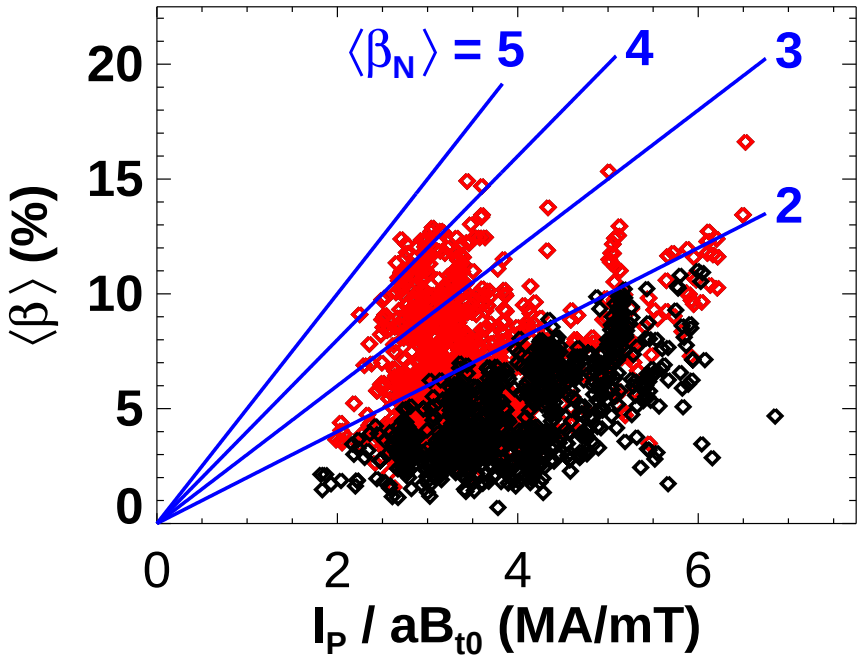

Figure 6:

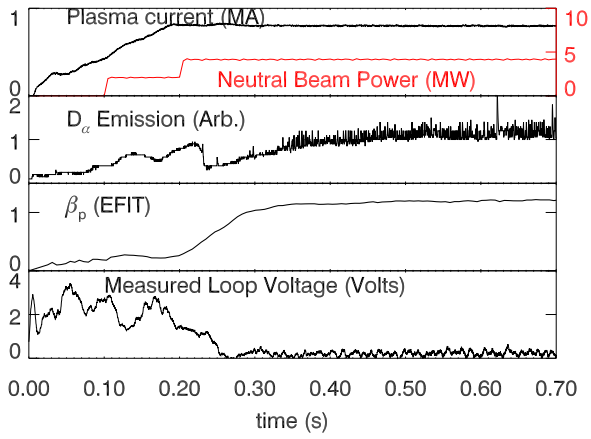
Plasma current (MA)
Neutral Beam Power (MW)
D$_\alpha$ Emission (Arb.)
β_p (EFIT)
Measured Loop Voltage (Volts)
time (s)

Figure 7:

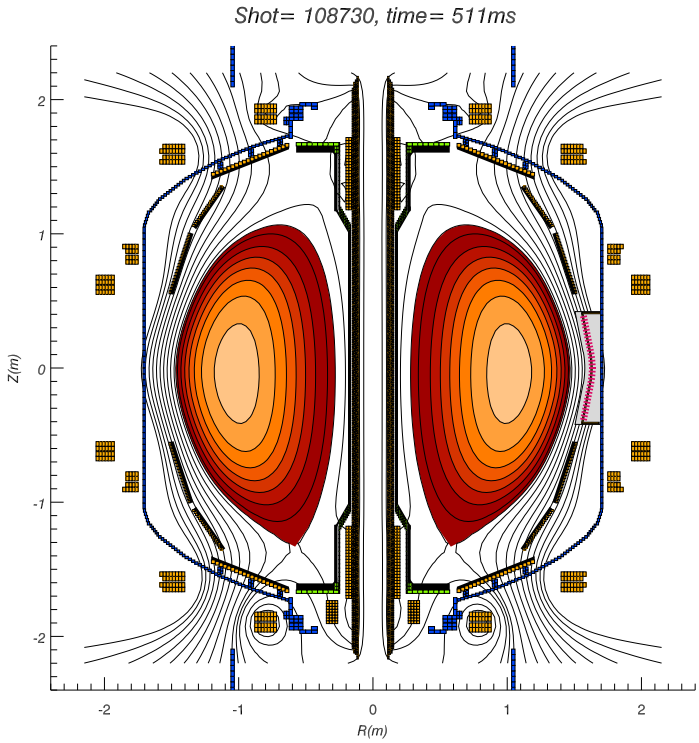

Figure 8:

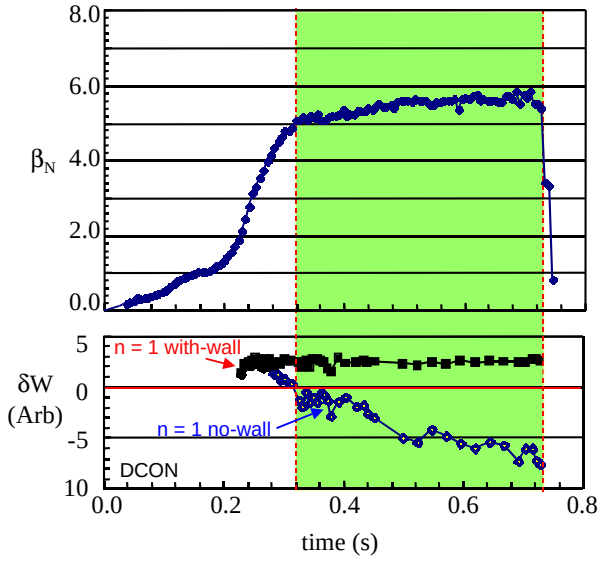
8.0
6.0
β_N 4.0
2.0
0.0
5
δW
(Arb) 0
-5
10
n = 1 with-wall
n = 1 no-wall
DCON
0.0
0.2
0.4
0.6
0.8
time (s)

Figure 9:

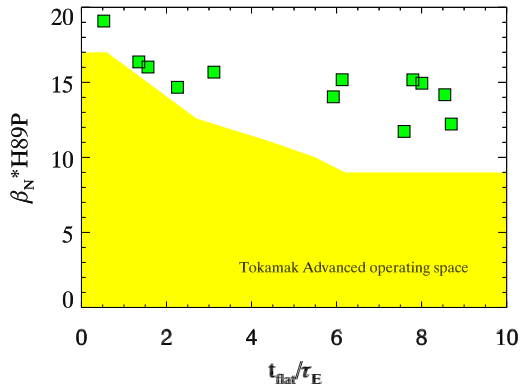

Figure 10: Database of NSTX discharges with high $\beta_N * H_{89P}$ plotted vs. the normalized time for which $\beta_N * H_{89P}$ was maintained. Time is normalized to the energy confinement time.

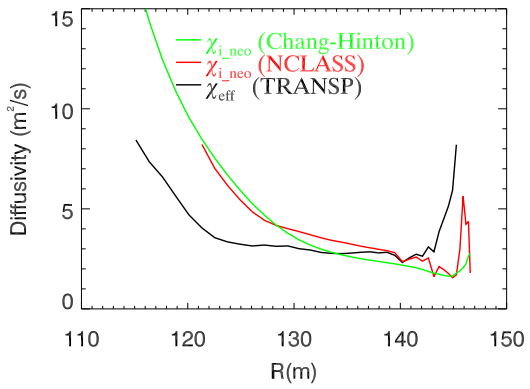
15
10
5
0
110
120
130
140
150
R(m)
Diffusivity (m²/s)
χi_neo (Chang-Hinton)
χi_neo (NCLASS)
χeff (TRANSP)

Figure 11:

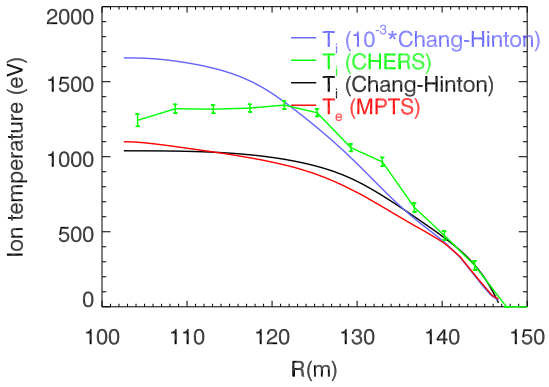
2000
1500
1000
500
0
Ion temperature (eV)
100
110
120
130
140
150
R(m)
T_i (10^-3*Chang-Hinton)
T_i (CHERS)
T_i (Chang-Hinton)
T_e (MPTS)

Figure 12: